

原子ビーム法による 低速不安定核ビーム生成に向けた 開発研究

理研・旭応用原子核物理研究室
亀田大輔

発表の流れ:

- 1、中性子過剰核のモーメント測定
- 2、低速不安定核ビームR&D
 - 減速材の開発
 - ABR、ABLS
- 3、まとめ

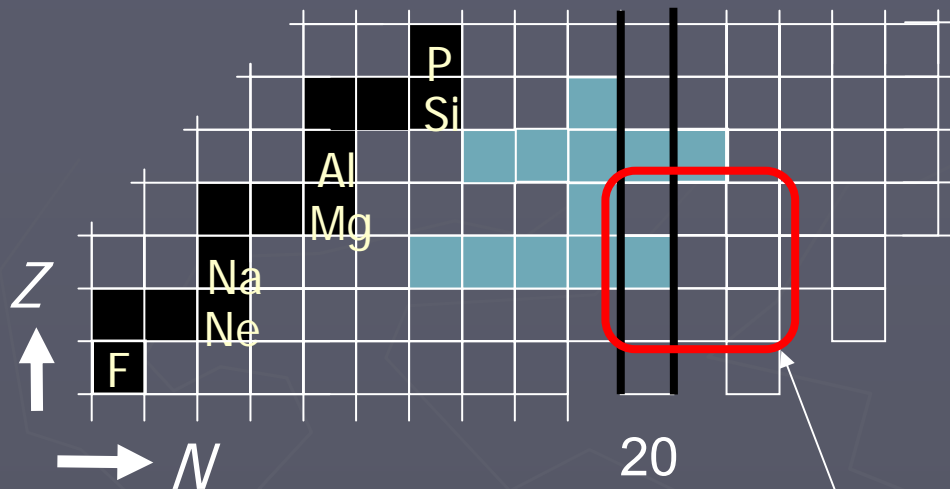
RIKEN Nishina center for Accelerator based science
上野秀樹, 吉見彰洋, 杉本崇, 旭耕一郎

Department of Physics, Tokyo Institute of Technology
島田健司, 長江大輔

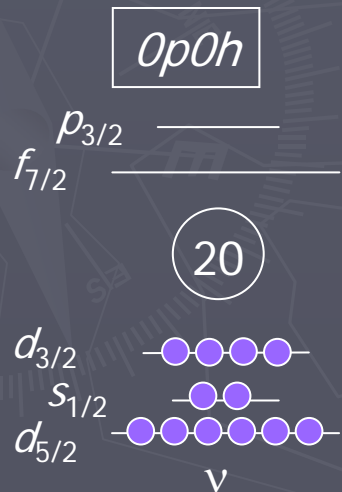
Rikkyo University
村田次郎, 川村広和



Nuclear moment studies around the island of inversion



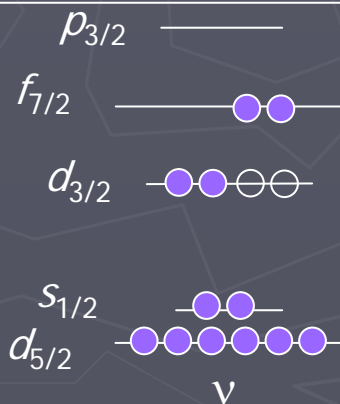
Normal *sd*-shell configuration



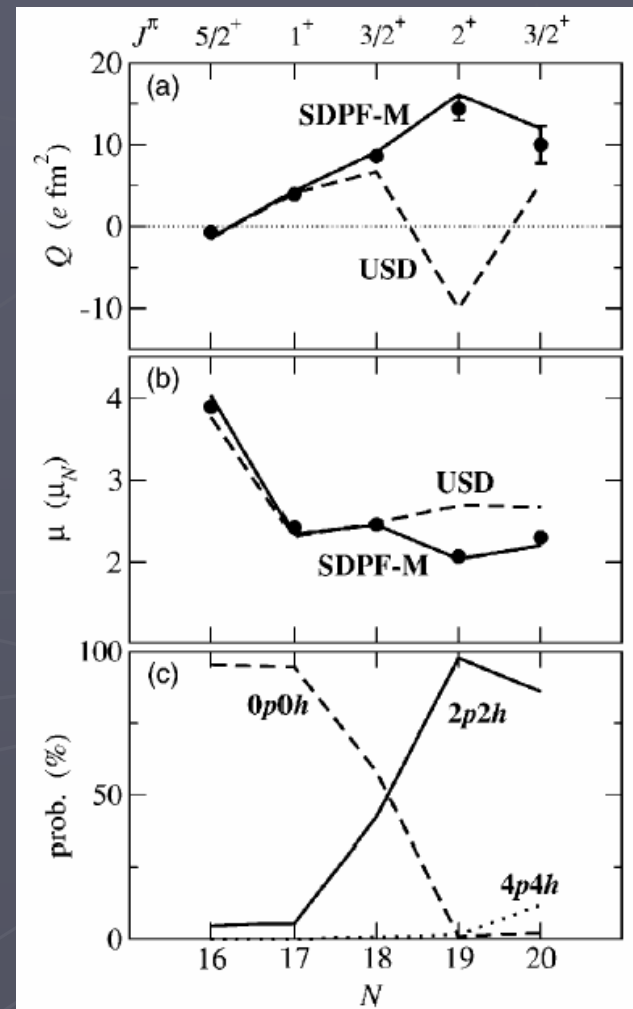
Island of Inversion

E.K. Warburton, J. A. Becker and B. A. Brown, PRC41(1990)1147.

2p2h (intruder), deformed

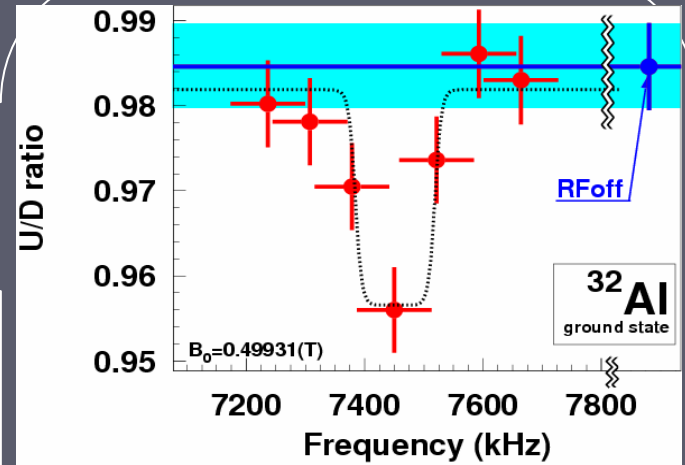
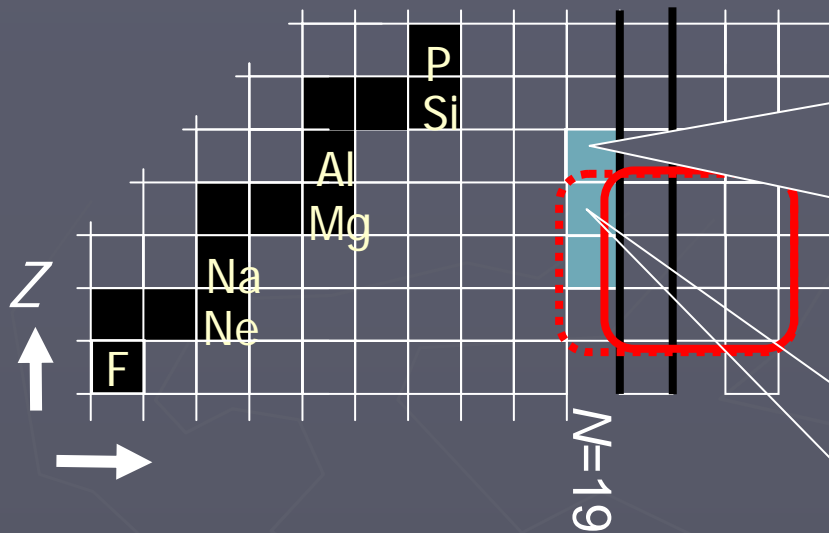


Nuclear moments of Na isotope chain:



Monte Carlo shell model with *sdpf* model space: Y. Utsuno, *et al.*, Phys. Rev. C70(2004) 044307.

Magnetic moment studies on neutron-rich $N=19$ isotones



$|\mu(^{32}\text{Al}_{\text{gs}}; 1^+)| = 1.959(9) \mu_N$
 ... well reproduced by sd ($0p0h$) shell models
 H. Ueno et al, PLB615 (2005)186.

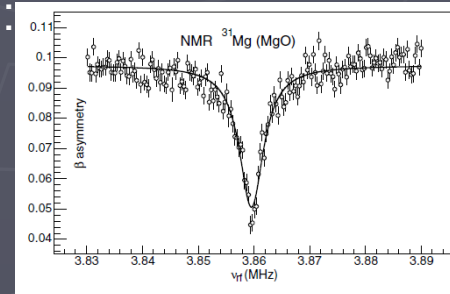
$^{32}\text{Al}_{\text{g.s.}}$:

1. ~~dominated by a $2p2h$ state~~
2. $\sim 50\%$ mixing of a $2p2h$ state to a $0p0h$ state
3. dominated by a $0p0h$ state

The Q -moment for the ground state of ^{32}Al is expected to provide the conclusive answer.

$\mu(^{31}\text{Mg}, I^\pi=1/2^+)$:
 $\rightarrow 2p2h$, deformed

G. Neyens *et al.*,
 Phys. Rev. Lett. 94
 (2005) 022501.

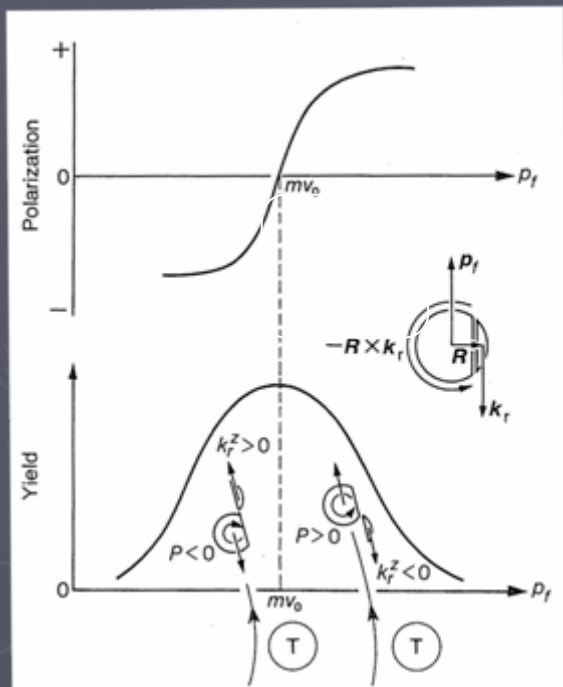


^{32}Al のQモーメント測定

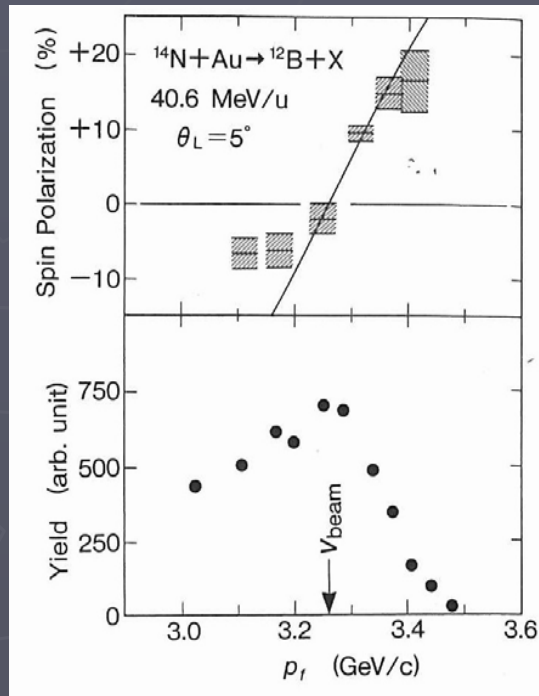


入射核破碎反応による スピン偏極不安定核ビームの生成

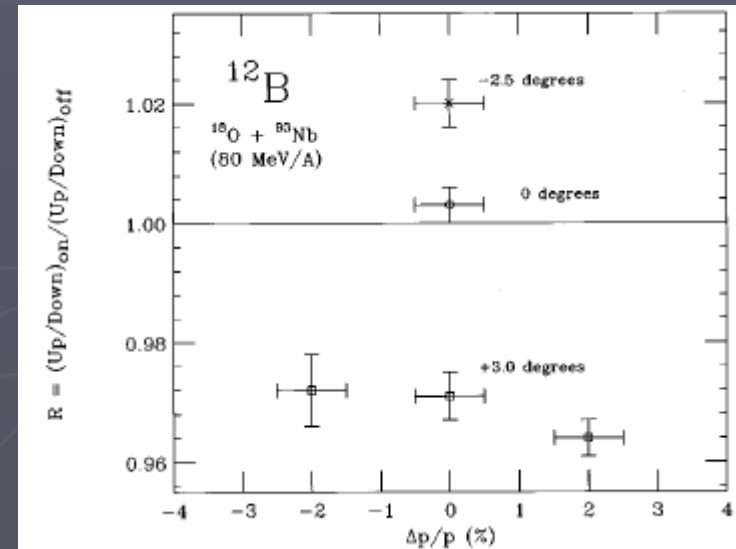
Kinematical model



Experiment



^{18}O (80 MeV/A) + $^{93}\text{Nb} \rightarrow ^{12}\text{B}$:
6-nucleon removals

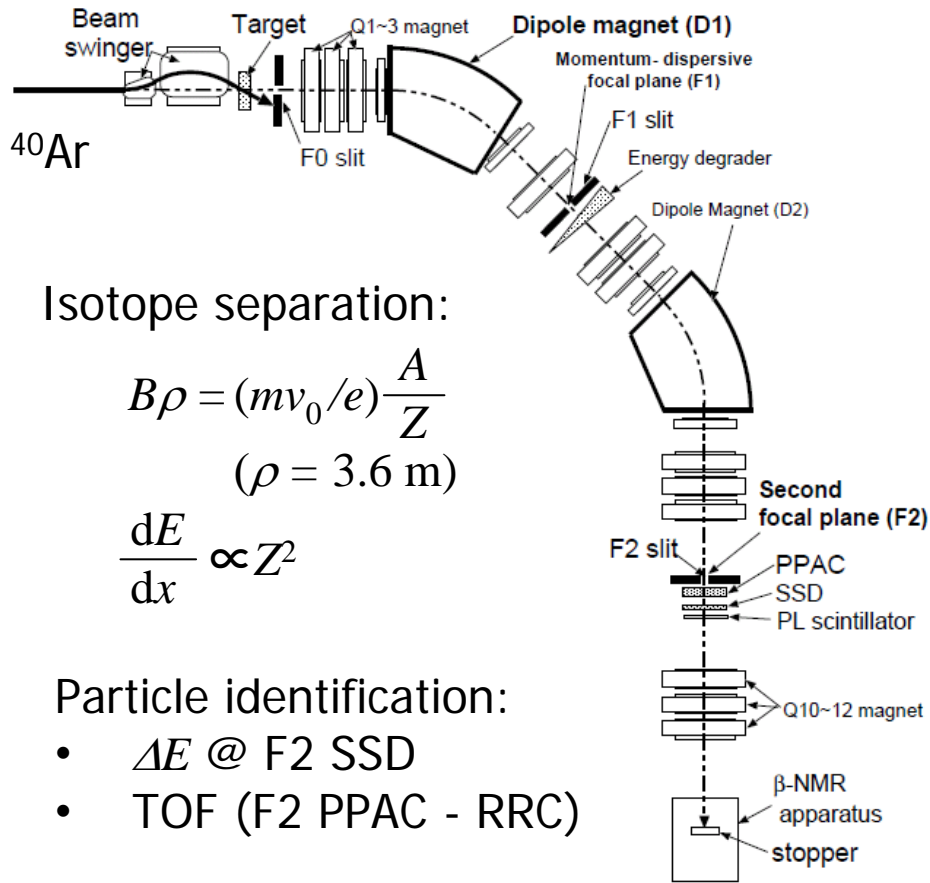


K. Asahi *et al.*,
Phys. Lett. B251 (1990) 488

P.F. Mantica et al.,
Phys. Rev. C55 (1997) 2501

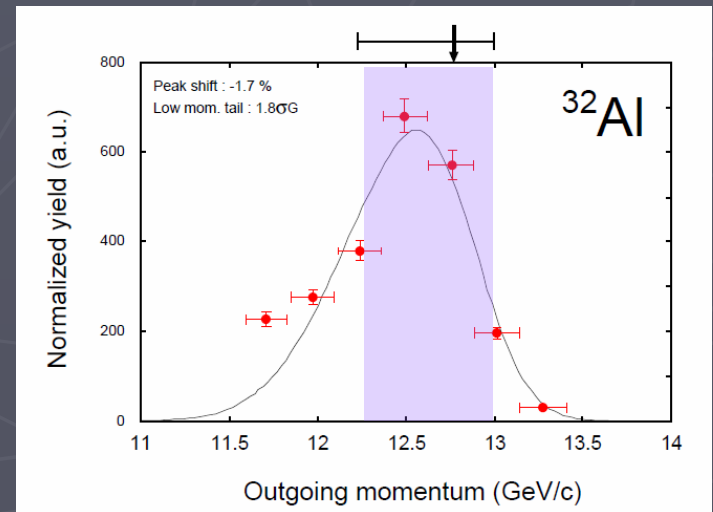
Production of spin-polarized ^{32}Al beam

RIKEN Projectile fragment separator (RIPS):

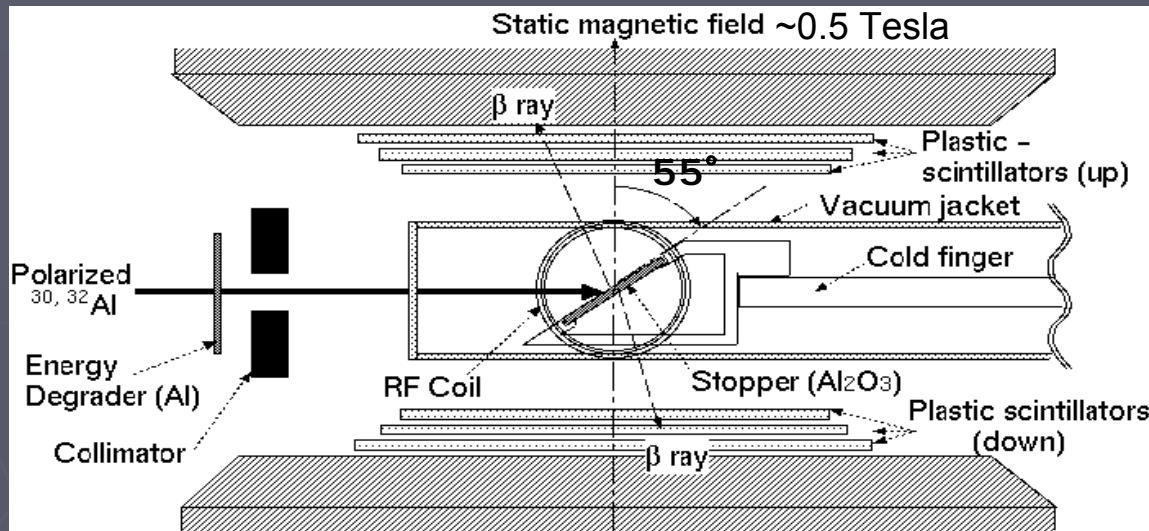


| | |
|----------------|-------------------------------|
| Primary beam | ^{40}Ar |
| | 95 AMeV, 40pnA |
| Nb target | Nb, 0.37 g/cm ² |
| Secondary beam | ^{32}Al |
| Emission angle | 1.3 – 5.2 deg. |
| Momentum | 12.6 GeV/c \pm 3 % |
| Intensity@F2 | 5×10^3 particle/sec. |
| Purity | 85% |
| Polarization | ~ 0.7 % |

Selected momentum region:



β -NMR apparatus:

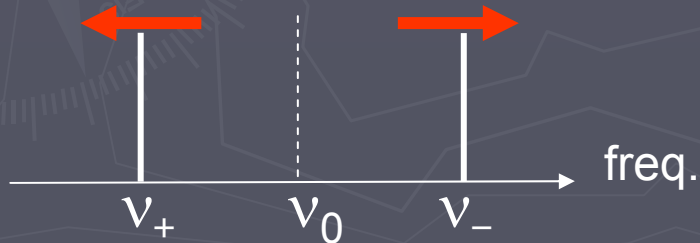


The resonance frequencies of $^{32}\text{Al}(I=1)$ in a stopper of **single-crystal $\alpha\text{-Al}_2\text{O}_3$** :

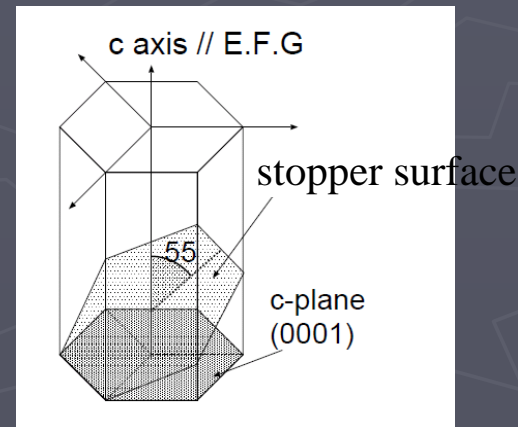
$$\nu_{\pm} = \nu_0 \mp \frac{3\nu_Q}{4} \frac{3 \cos^2 \theta_c - 1}{2}$$

$$\nu_0 = g\mu_N B_0 / h \quad (\text{Larmor frequency})$$

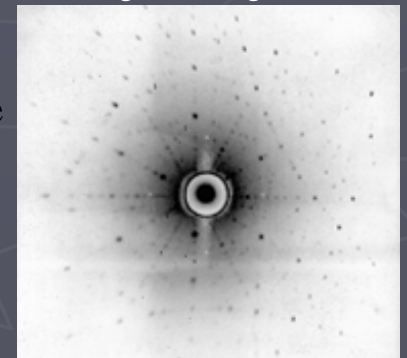
$$\nu_Q = e^2 q Q / h \quad (\text{Quadrupole coup. const.})$$



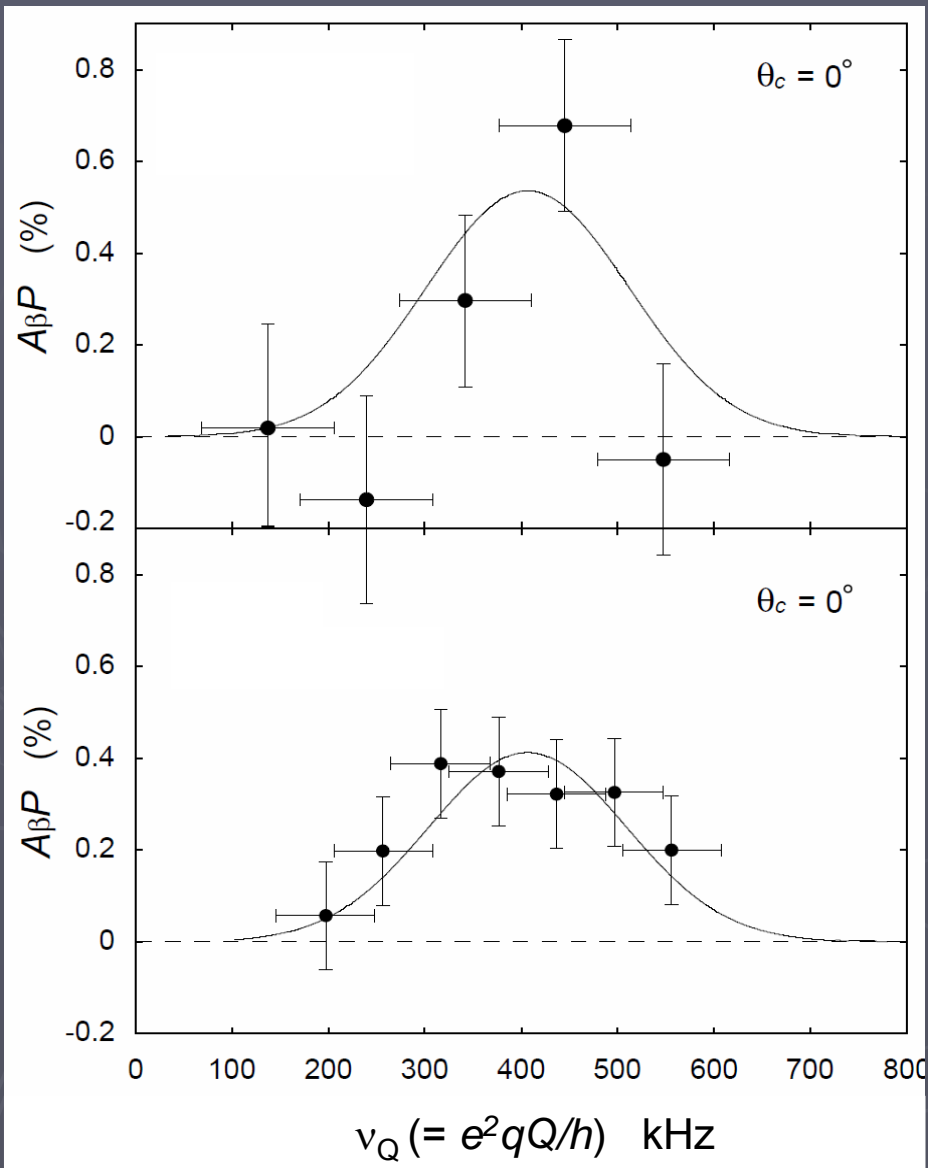
Crystal structure of $\alpha\text{-Al}_2\text{O}_3$: h.c.p.



X-ray analysis



Quadrupole resonance spectra with $\alpha\text{-Al}_2\text{O}_3$ stopper



Stopper conditions:

- Crystal c -axis $\parallel B_0$
- Temperature ~ 80 K

Analysis :

- Fitting: gaussian including AFP effect
- Chemical shift correction: 0.00188(3) %
J. Magn. Reson. 128 (1997) 135.

Result : $\nu_Q(^{32}\text{Al}) = 407(34)$ kHz

$$\frac{|Q(^{32}\text{Al})|}{\nu_Q(^{32}\text{Al})} = \frac{|Q(^{27}\text{Al})|}{\nu_Q(^{27}\text{Al})} = \frac{140.2(10) \text{ mb}}{2389(2) \text{ kHz}}$$

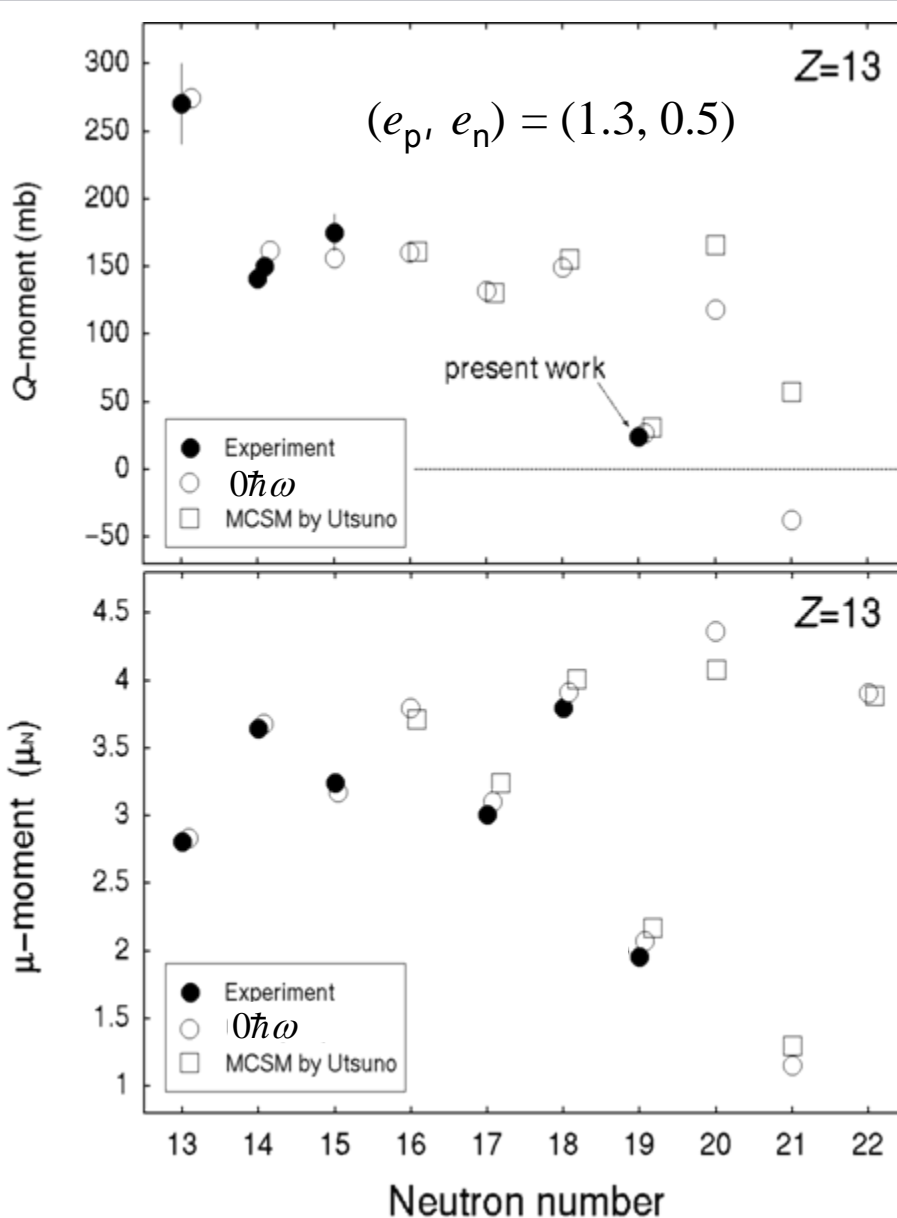
ref. $\nu_Q(^{27}\text{Al})$ in $\alpha\text{-Al}_2\text{O}_3$:

J. Magn. Reson. **89** (1990) 515.

$Q(^{27}\text{Al})$: Phys. Rev. Lett. **68** (1992) 927.

$$|Q(^{32}\text{Al})| = 24(2) \text{ mb}$$

Systematic comparison : μ and Q for Al isotopes



$0\hbar\omega$ shell model calculations:

- USD effective interaction
- effective operators

B. Wildenthal, Prog. Part. Nucl. Phys. **11** (1984) 5

B.A. Brown and B.H. Wildenthal, Nucl. Phys. A **474** (1987) 290

sd wave function for $^{32}\text{Al}_{\text{g.s.}}$:

$$|^{32}\text{Al}_{\text{g.s.}}(I^\pi=1^+)\rangle = \alpha |\pi d_{5/2}^{-1} \nu d_{3/2}^{-1}\rangle^{J=1^+} + \beta |\pi(d_{5/2}^3 d_{3/2}^2) \nu d_{3/2}^{-1}\rangle^{J=1^+} + \dots$$

$$\alpha^2 = 79\%, \quad \beta^2 < 3.8\%$$

Large-scale shell model calculations by Utsuno in private comm.

$^{32}\text{Al}_{\text{g.s.}}$: sd -normal configurations : 87 %
 fp-intruder configurations : 13 %

$^{32}\text{Al}_{\text{g.s.}}$:

- ~~1. dominated by a $2p2h$ state~~
- ~~2. ~50% mixing of a $2p2h$ state to a $0p0h$ state~~
- 3. dominated by the $0h0p$ state**

Studies on the neutron-rich N=19 isotones:

^{33}Si ($Z=14$) \rightarrow sd shell structure (normal)

Reaction study

L.K. Fifield et al., Nucl. Phys. A453, 497 (1986).
B. Fornal et al., Phys. Rev. C 49, 2413 (1994).
B.V. Pritychenko et al., Phys. Rev. C 62, 051601(R) (2000).
J. Enders et al., Phys. Rev. C 65, 034318 (2002).
A.C. Morton et al., Phys. Lett. B 544, 274 (2002).

β - γ spectroscopy

^{32}Al ($Z=13$) \rightarrow normal sd-shell or pf-intruder ?

Reaction

β - γ

β -n

Isomer production via PF

μ -moment for g.s.

Q-moment for g.s.

B. Fornal et al., Phys. Rev. C 55, 762 (1996).
G. Klotz et al., Phys. Rev. C 47, 2502 (1993).
S. Grevy et al., Nucl. Phys. A 734, 369 (2004).
M. Langevin et al., Nucl. Phys. A 414, 151 (1984).
M. Robinson et al., Phys. Rev. C 52, R1465 (1996).
H. Ueno et al., Phys. Lett. B 615, 186 (2005).
D. Kameda et al., Phys. Lett. B, accepted (2007).

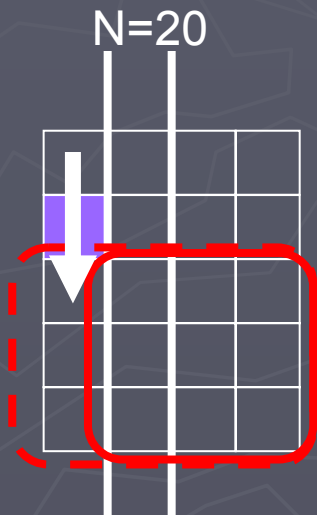
^{31}Mg ($Z=12$) \rightarrow deformed pf-intruder structure

Reaction

β - γ

μ -moment & spin

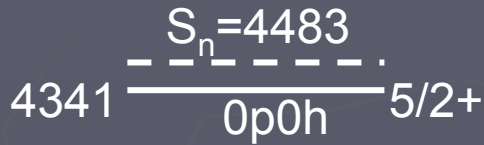
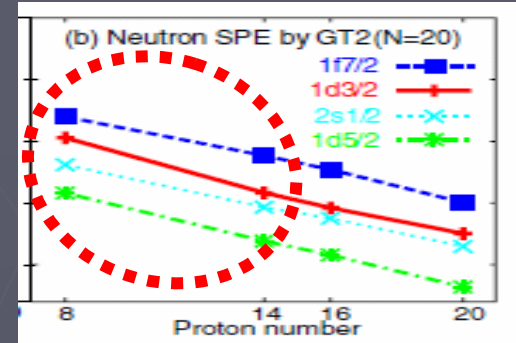
H. Mach et al., Eur. Phys. J. A 25, 105 (2005).
G. Klotz et al., Phys. Rev. C 47, 2502 (1993).
F. Marechal et al., Phys. Rev. C 72, 044313 (2005).
G. Neyens et al., Phys. Rev. Lett 94, 022501 (2005).



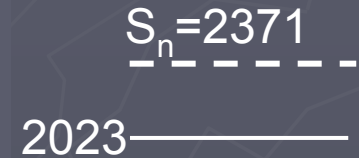
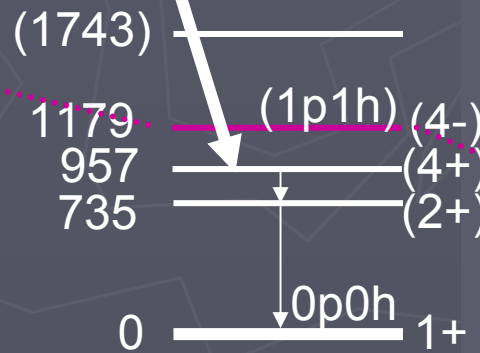
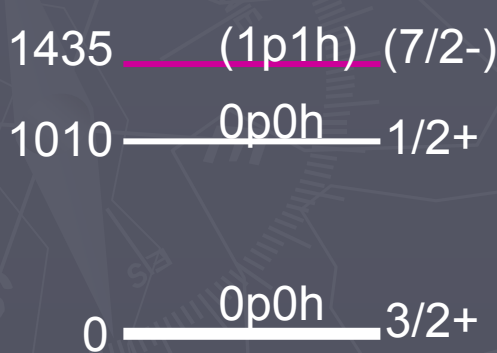
What happens in the $N=19$ low-lying levels ?

**Gradual reduction of the sd - pf shell gap
 → Coexistence of the npn h states ($n=0,1,2,\dots$)**

T. Otsuka et al.,
 PRL97(2006)162501



Isomer ($T_{1/2}=200$ ns)

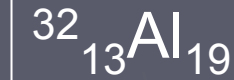


$^{33}_{14}\text{Si}_{19}$

$^{32}_{13}\text{Al}_{19}$

$^{31}_{12}\text{Mg}_{19}$

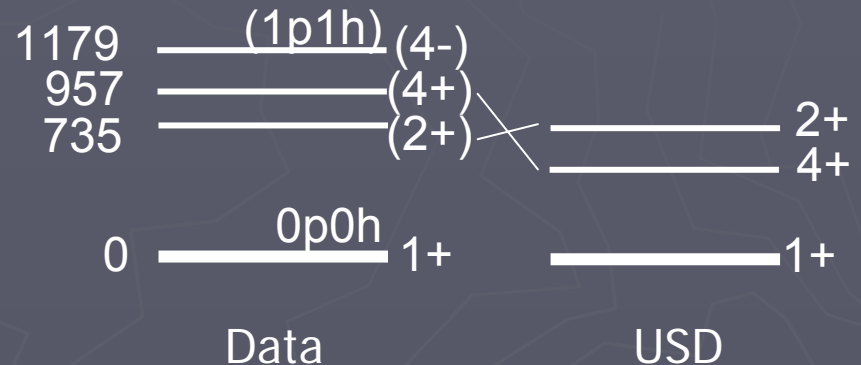
Nuclear moments of ^{32}mAl



Approach I:

Measurement of the isomeric μ - and Q - moments of ^{32}Al by the Time Differential Perturbed Angular Distribution (TDPAD) method:

- The spin/parity of the isomeric state
- The (mixing) amplitudes of the n p- n h ($n=0,2$) configurations



Approach II:

^{32}Mg β -delayed γ spectroscopy:

- β branching ratios, in particular, for the ground state of ^{32}Al
- Construct the level scheme

Submitted to RIBF proposal

| ^{32}Al | USD | EXP. |
|--------------------------------|---------|--------------|
| $g(4^+)$ | 1.330 | To be measu. |
| $g(2^+)$ | 1.628 | |
| $Q(4^+)$ | 163 mb | To be measu. |
| $Q(2^+)$ | 14.8 mb | |
| $Q(1^+_{\text{g.s.}})$ | 26.8 mb | 24(2) mb |
| $g(1^+_{\text{g.s.}})$ | 2.065 | 1.959(9) |
| $T_{1/2}(4^+ \rightarrow 2^+)$ | 122 ns | 200(20) ns |
| $T_{1/2}(2^+ \rightarrow 1^+)$ | 0.31 ps | |

今後の目標・課題

今後の目標:

- 不安定核の系統的な核モーメントデータを得る
(基底状態、及び励起状態の核モーメントデータ)
→ 殻構造変容の解明

課題:

- Spin orientation (polarization, alignment)
 - ▶ Projectile fragmentation...?
- Stopper to preserve the orientation
- SN ratio in the radiation detection

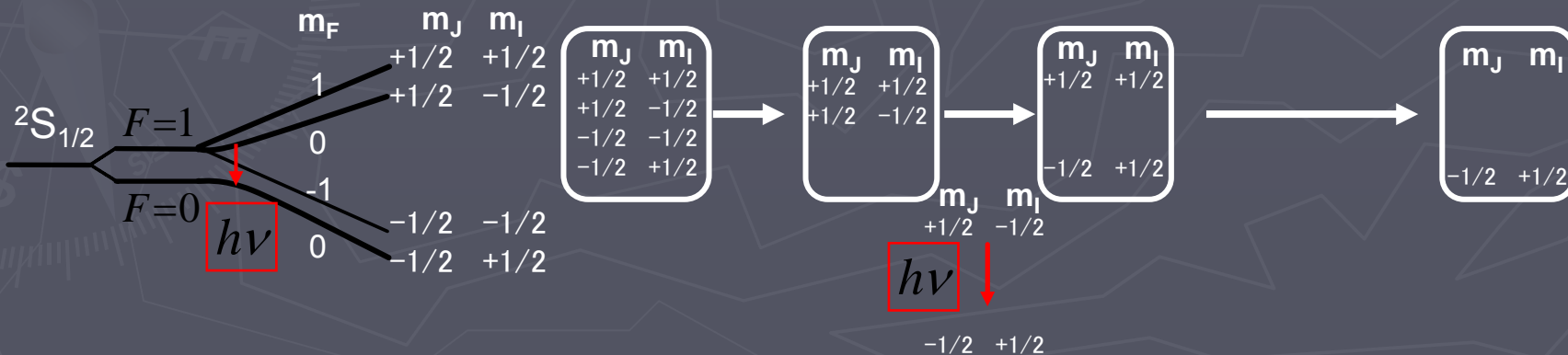
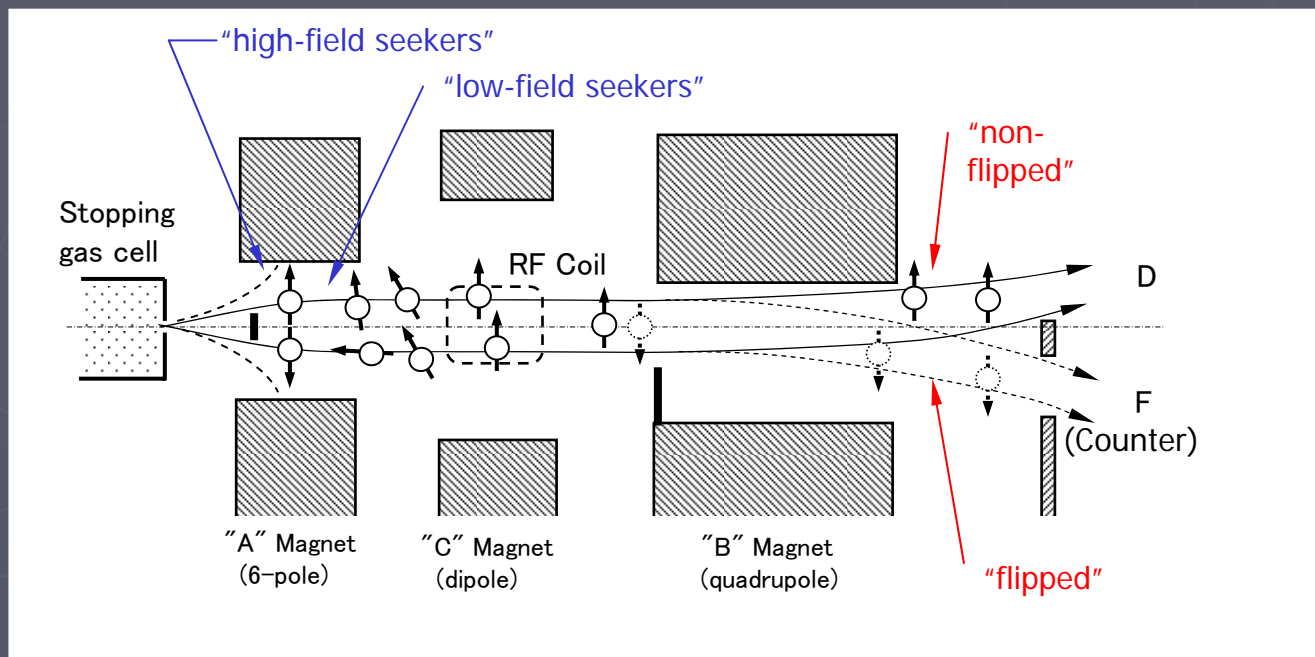
3S issues

in particular,
nuclear moment measurements of ground states

低速不安定核ビームを用いた核モーメント測定

→ Free from 3S issues

原子ビーム共鳴法:



低速不安定核ビームの生成過程

1. 減速: 減速材

- くさび状のアルミ板: 入射核破碎反応の運動量広がり補償
- Arガス: 圧力調整による厚さの微調整
- 両者の組み合わせ

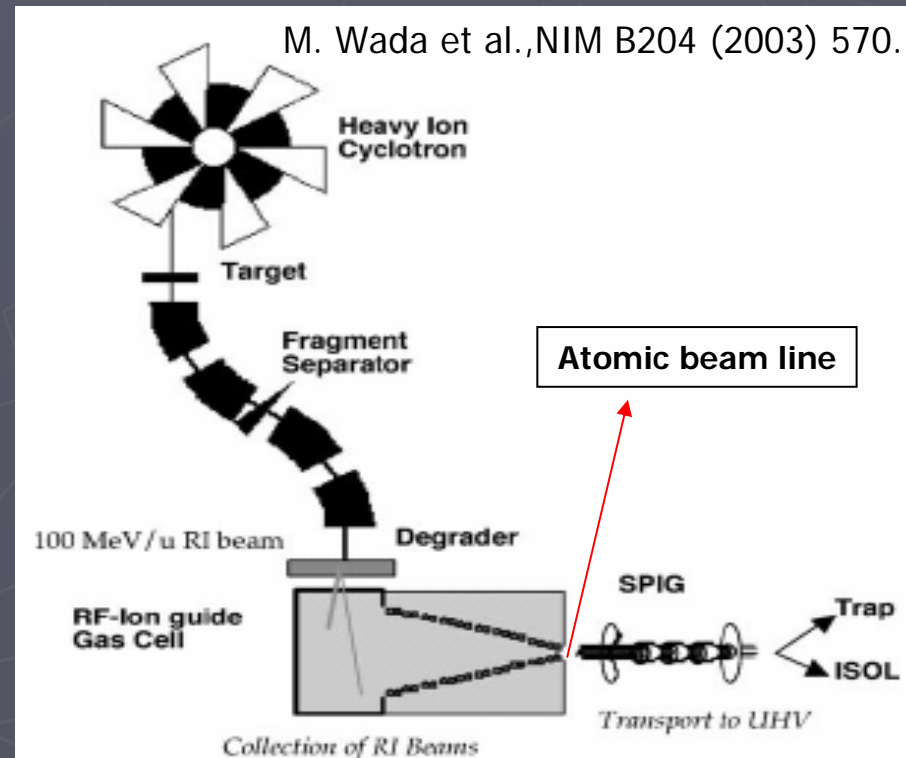
2. 停止 → 電場によるイオンの引き出し: 停止材ガス種

- Heガス: 非中性化効率大、ストップングパワー小
- Neガス: ストップングパワー大、非中性化効率...

3. 中性化

4. 原子ビーム生成

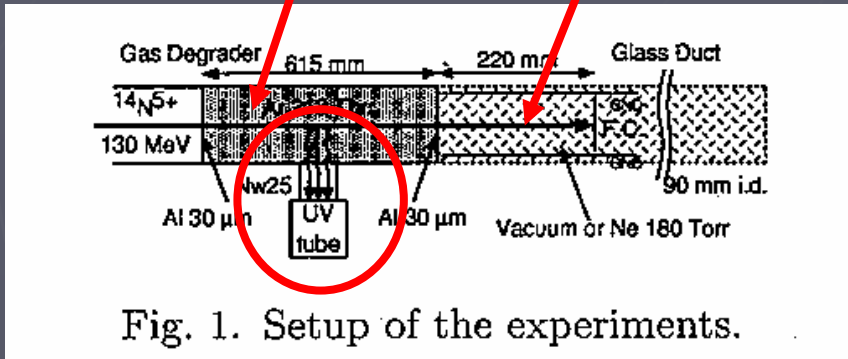
- ラバールノズル: 旧来方式



Arガス減衰層の開発@CYRIC

実験セットアップ

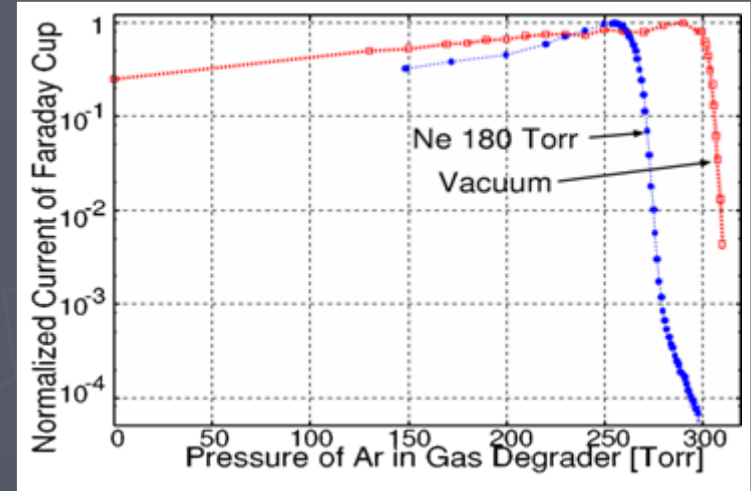
Ar-Gas degrader Ne-Gas stopper



- 入射ビーム: ^{14}N (Stable), 130MeV
- 減衰層(兼ビームモニター): Arガス
- ストッパー: Neガス

停止位置は、チャンバー内に置いたファラデーカップ(F. C.)の電流値より測定

Arガス圧調整 (F.C.固定位置):



ガ

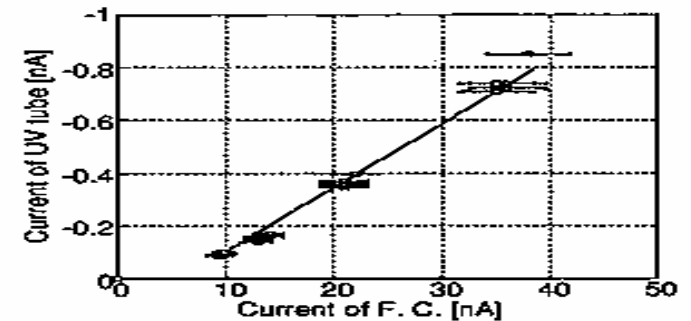
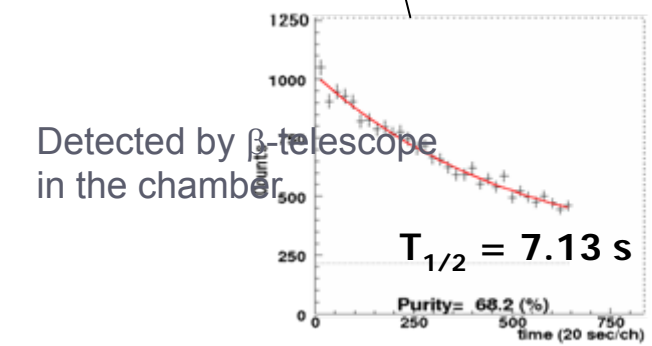
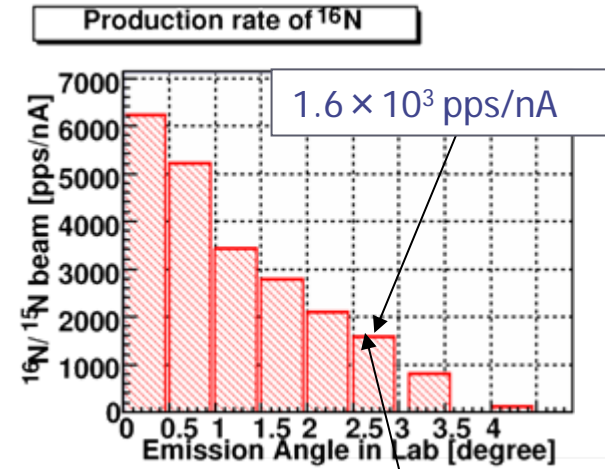
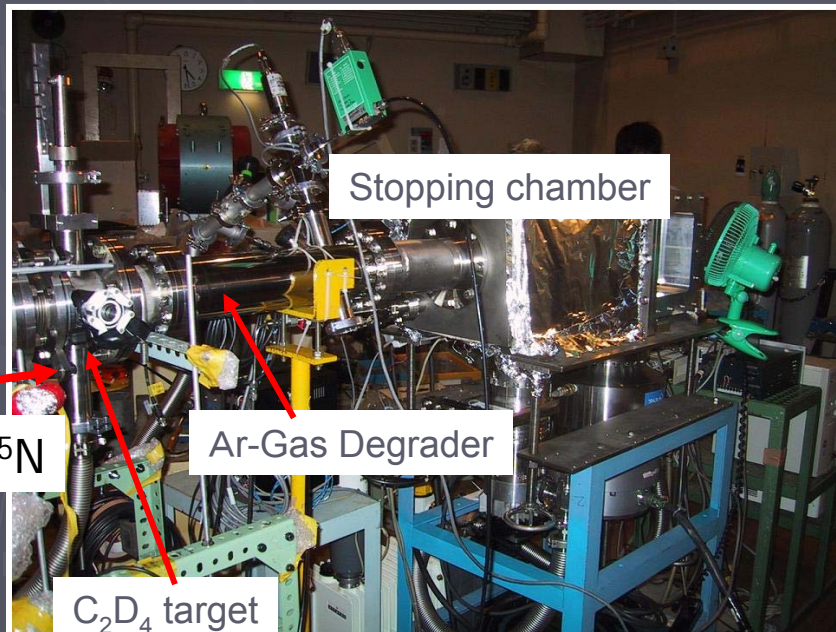
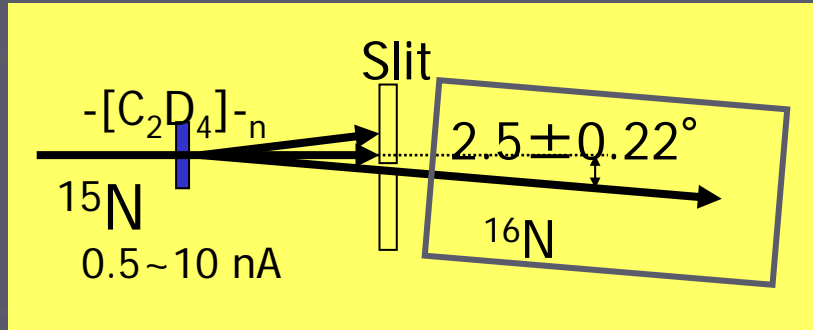


Fig. 3. Currents at the UV multiplier tube and F. C. were changing beam intensity.

不安定核ビームを用いた停止位置の確認@CYRIC

Production of ^{16}N ($l=1$, $T_{1/2}=7.1$ s)

$d(^{15}\text{N}, ^{16}\text{N})p$ @ Cyclotron Center, Tohoku Univ.

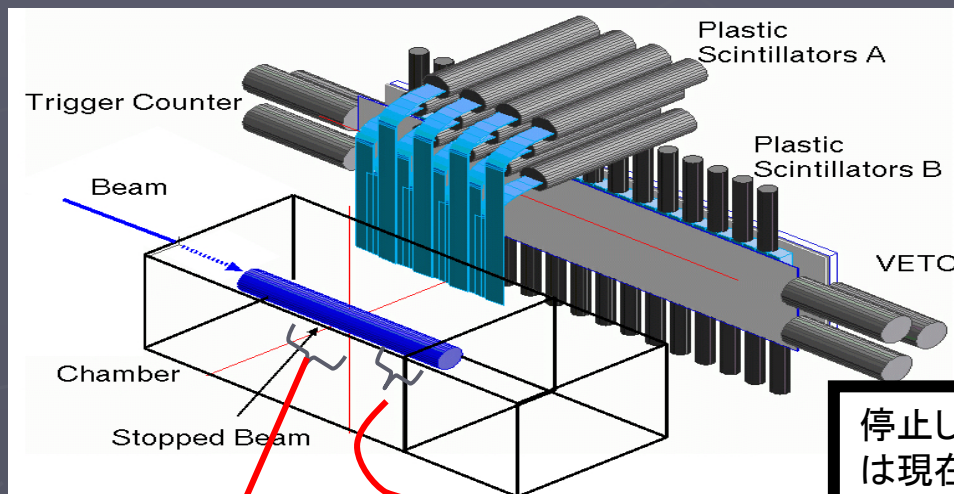


10^4 cps ^{16}N (with 10nA of ^{15}N)
 \rightarrow Extraction $\rightarrow 10^3$ cps
 \downarrow
 Experiment for extraction/neutralization is possible

Arガス圧による停止位置の微調整@CYRIC

入射ビームの停止分布測定

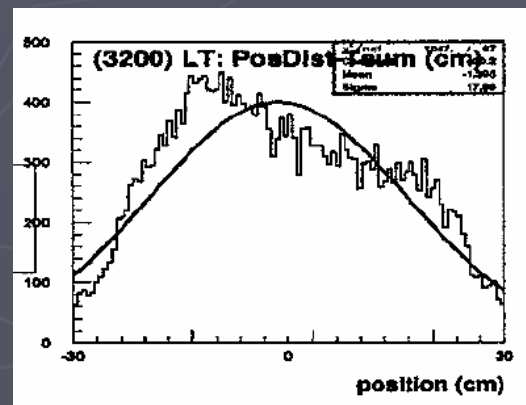
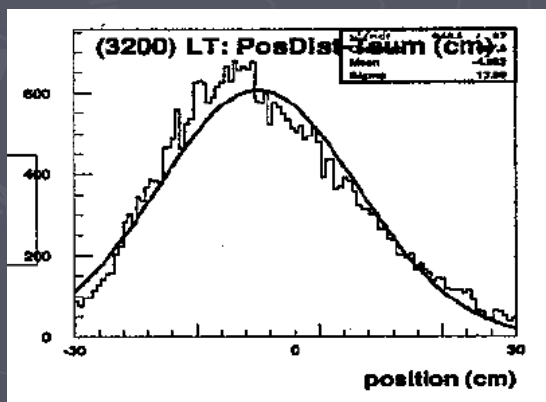
外側の β -telescope から ^{16}N 停止位置を観測



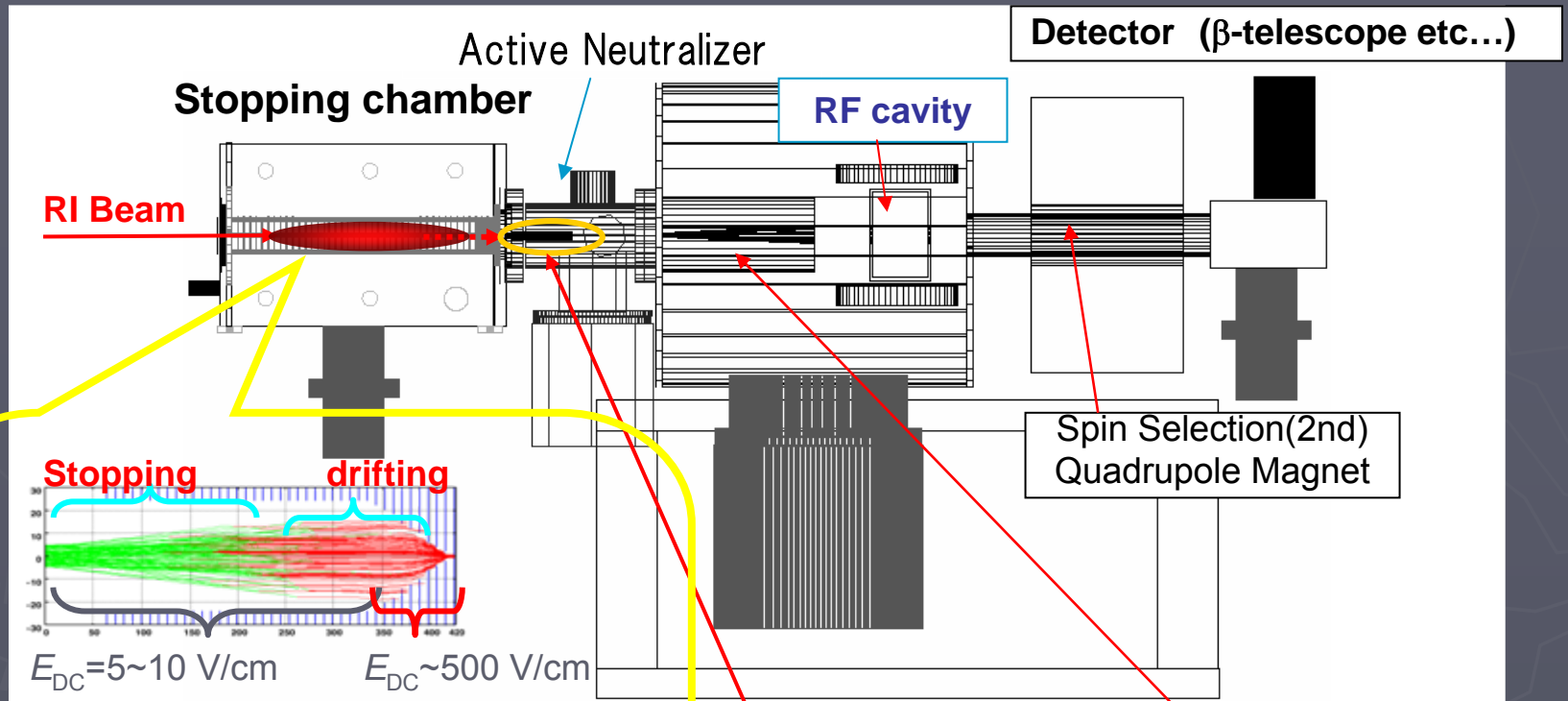
停止した ^{16}N の電場によるドリフトの確認は現在進行中...

中心付近に停止

ノズル付近に停止



低速不安定核ビームの応用I: 原子線共鳴法



Note:

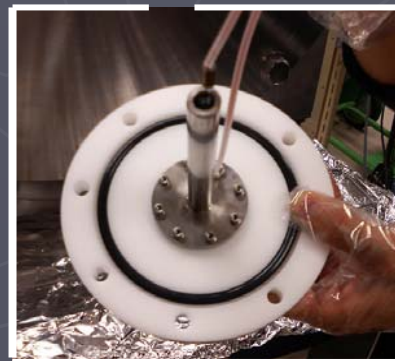
$$v_{ion} = \mu E_{DC} \quad \mu: \text{mobility}$$

$$\mu = 4.0 \text{ (in Ne gas)}$$

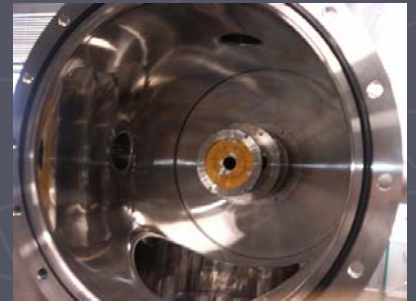
$$\mu = 10.0 \text{ (in He gas)}$$

120 ms for $E=10\text{V/cm}$, Ne 200 torr

Yttrium tube



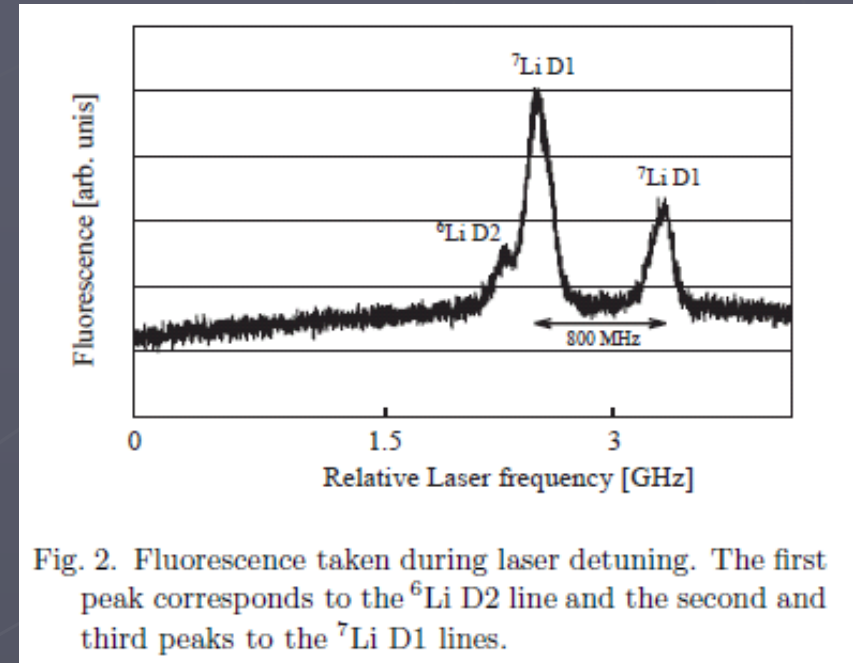
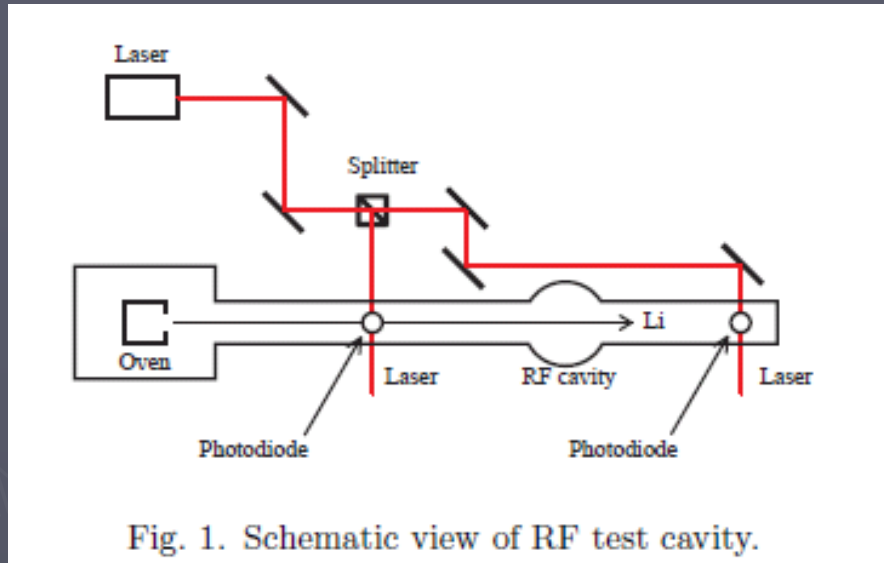
Spin Selection(1st) Sextupole Magnet



1.3T@pole tip

応用II: 原子線レーザー分光

オフライン開発段階:



${}^7\text{Li}$ atomic beam:

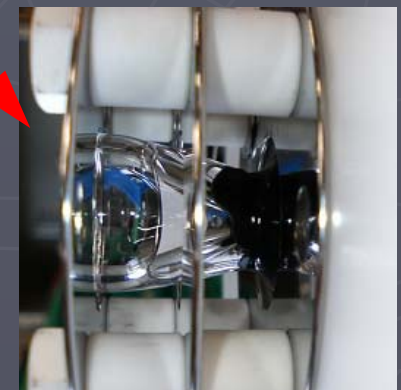
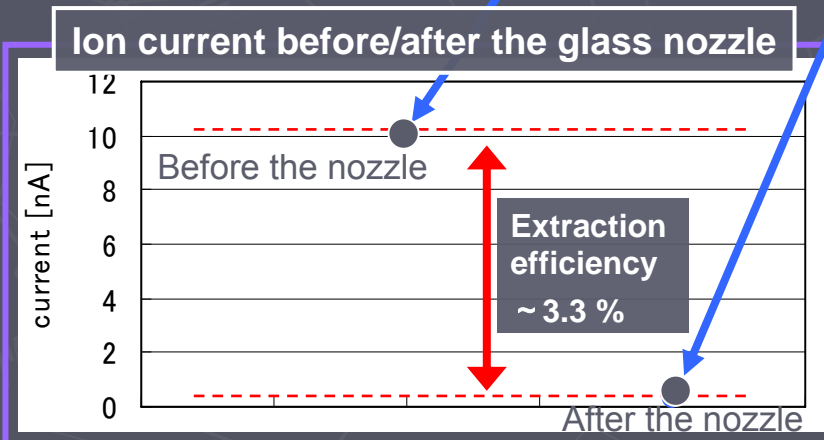
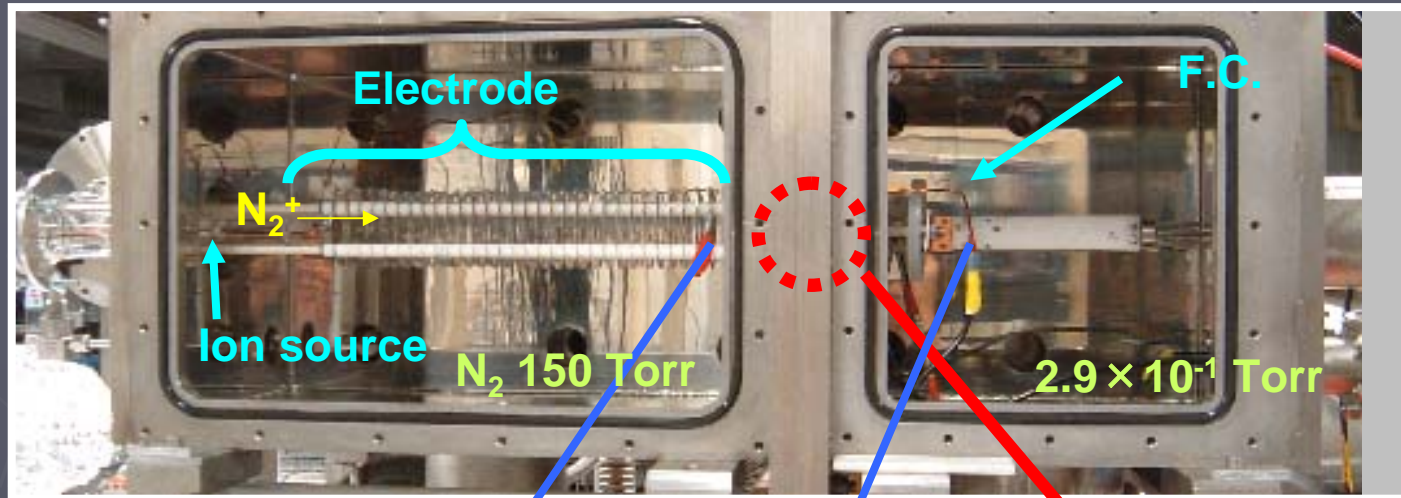
Optical pumping by a diode laser: ${}^2\text{S}_{1/2}, F=1 \rightarrow {}^2\text{P}_{1/2}, F=2$ (D1)

まとめ

- ▶ 不安定核の系統的な電磁気モーメントデータ
→ 不安定核構造を探る上で不可欠
- ▶ 3S課題の克服
 - 基底状態の核モーメント測定:
低速不安定核ビーム生成に向けた開発
不安定核ビームを用いた開発実験の必要性
 - アイソマーの核モーメント測定:
TDPAD, TDPAC, etc...

オフライン: イオンの引き出し

放電による生成イオンを用いて、オフライン実験を行った

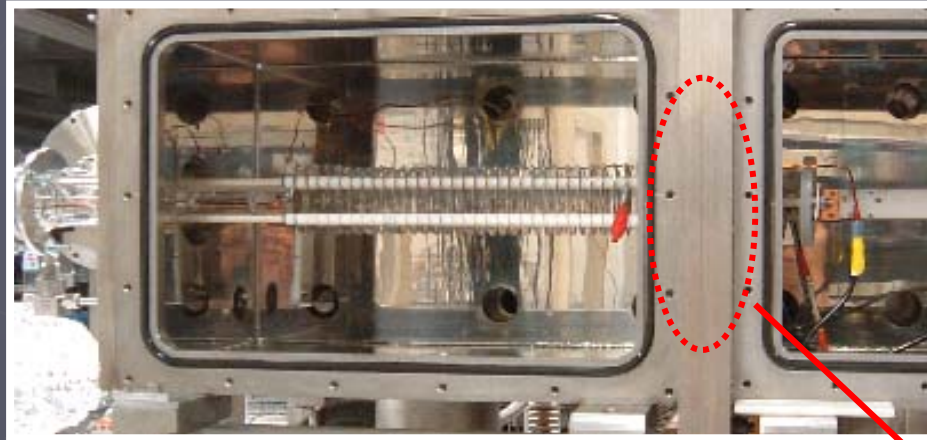


Glass nozzle $\Phi 1$ mm (Laval-type)

オフライン:RF イオンガイド

イオンの引き出しを向上するために.....

Ion-guide efficiency = 33%
Wada et al., NIMA 532(2004)40



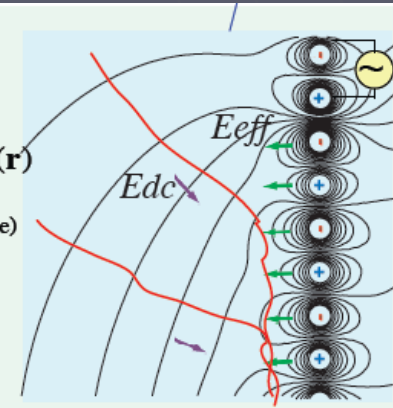
RF gradient Field:
 Barrier

$$\bar{F} = -\frac{e^2}{4m(\Omega^2 + 1/\tau_v^2)} \nabla E_{rf}^2(\mathbf{r})$$

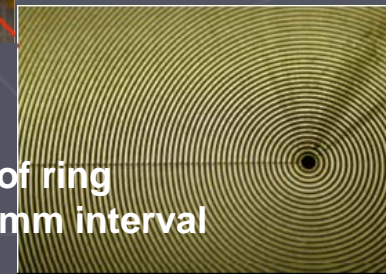
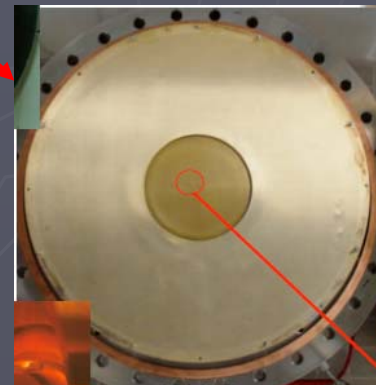
$(E(\mathbf{r},t) = E_{rf}(\mathbf{r}) \cos(\Omega t), \tau_v: \text{relax time})$

$$E_{\text{eff in gas}}^{\text{max}} = \frac{m\mu^2 V_{rf}^2}{er_0^3}$$

$2r_0 \approx \text{electrode distance}$



Off-line experiments with LASER-induced ions
 → On-line experiments with 16N beam (2006/12, 2007/1-2)



Carpet is made of ring electrodes 0.28 mm interval

軽核領域の核モーメント測定

TITech / RIKEN

Osaka / RIKEN

• g -Factors measured at RIKEN

- Boron isotopes : ^{14}B , ^{15}B , ^{17}B
- Carbon isotopes : ^9C , ^{15}C , ^{17}C
- Nitrogen isotopes : ^{17}N , ^{18}N , ^{19}N
- Oxygen isotopes : ^{13}O
- Fluorine isotopes : ^{21}F
- Aluminum isotopes: ^{23}Al , ^{30}Al , ^{32}Al

Spin-parity
assignment

Effect of neutron excess
on the magnetic moment

• Q -moments measured at RIKEN

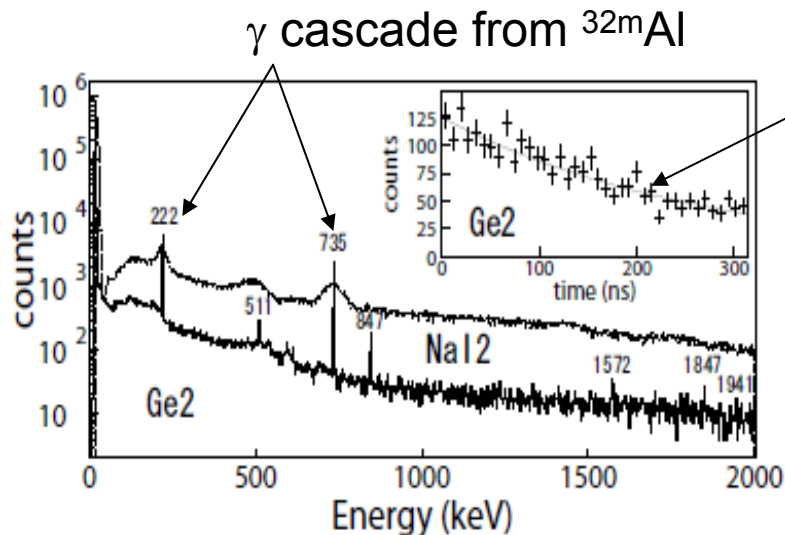
- Boron isotopes : ^{14}B , ^{15}B , ^{17}B
- Nitrogen isotopes : ^{18}N
- Oxygen isotopes : ^{13}O
- Magnesium isotopes : ^{23}Mg
- Aluminum isotopes: ^{31}Al , ^{32}Al

Reduction of $E2$ effective
charges

I, TDPAD measurements

1. Produce spin-aligned ^{32}Al isomers
 - Projectile fragmentation of ^{40}Ar (95 MeV/u)
2. Implant the isomers in a stopper
 - g-factor: Perturbation-free material, metal(Al, Cu), MgO, Si
 - Q-moment: $\alpha\text{-Al}_2\text{O}_3$ (The E.F.G. was known)
3. Detect the γ -ray decay of the isomeric state
 - Particle- γ slow coincidence technique
 - A static magnetic field with a suitable magnitude

We have already produced the $^{32\text{m}}\text{Al}$ beam in RIPS:

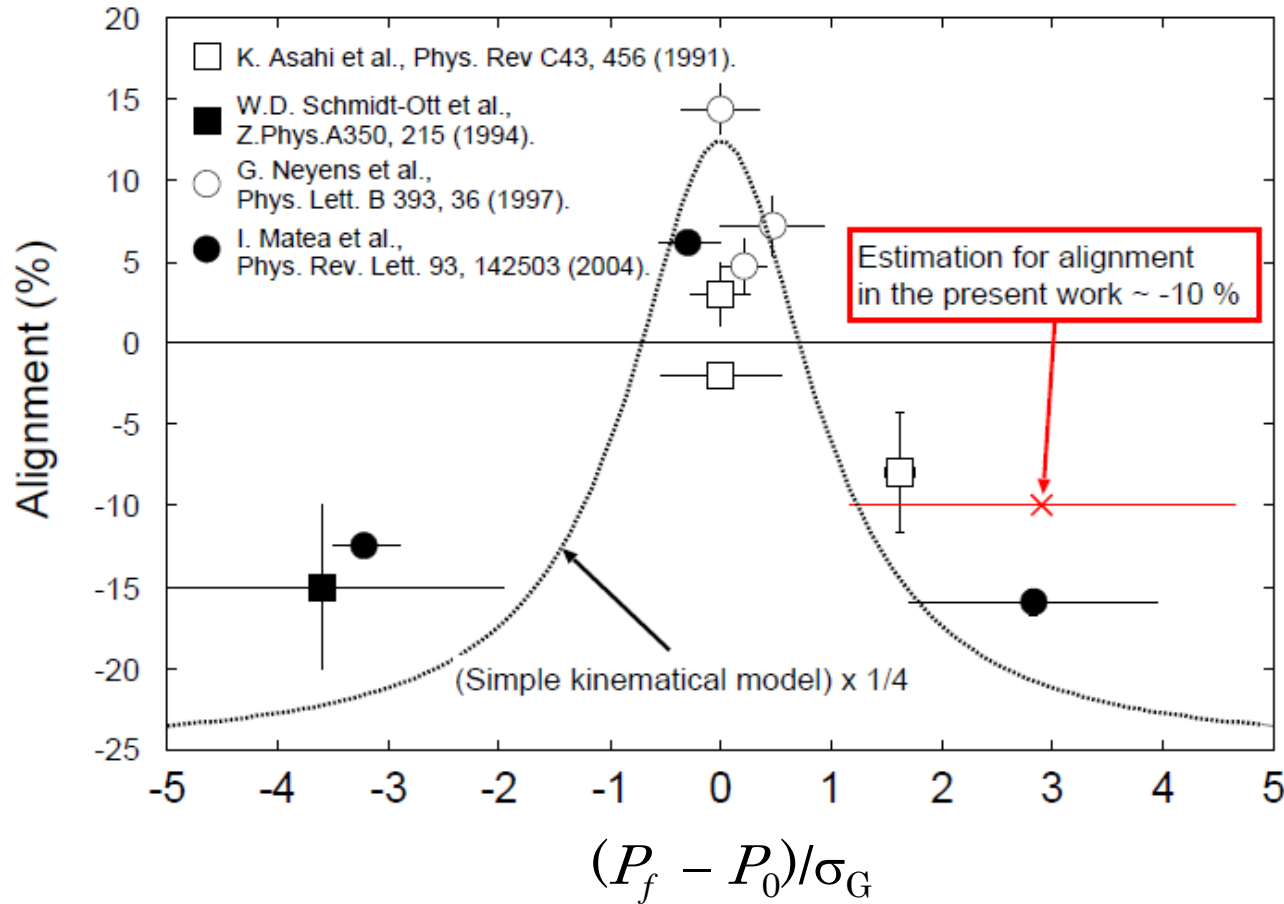


$$T_{1/2} = 199(10)\text{ns}$$

in good agreement with the literature
Background at the low-energy peak:

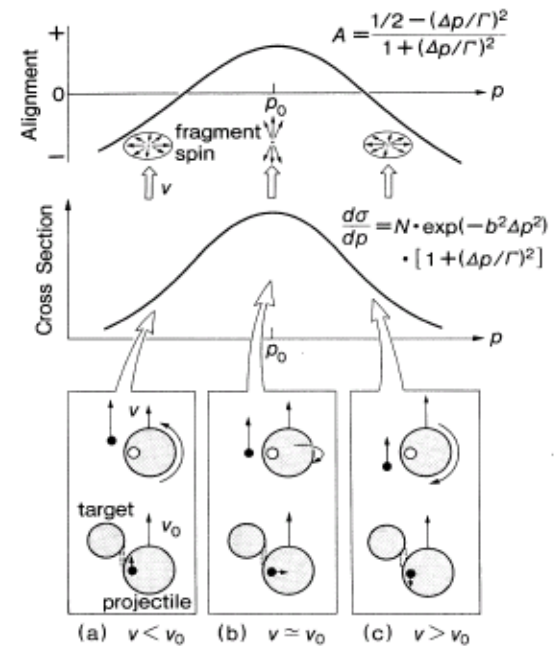
| | NaI | HPGe |
|----------------------|-----|------|
| SN ratio @222 keV | 1.3 | 30 |

Alignment via projectile fragmentation



Kinematical model:

K. Asahi et al., PRC43(1991)456.



Goldhaber distribution:

$$\sigma_G = \sigma_0 \sqrt{(A_f(A_p - A_f))/(A_p - 1)}$$

($\sigma_0 = 90 \text{ MeV}/c$)

A.S. Goldhaber, PLB53 (1974) 306.

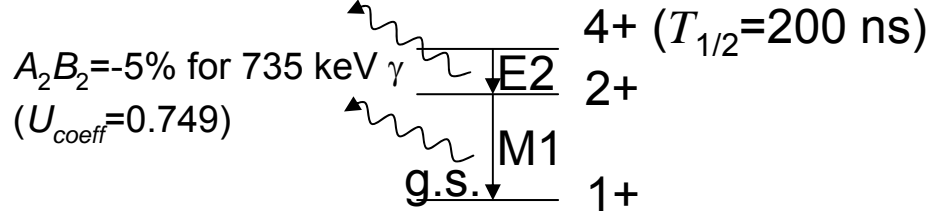
Simulation of TDPAD spectra by GEANT3

- Isomer yield = 1 kpps
- Alignment = - 10 %
- $g(^{32m}\text{Al})=1.33$
- Angular distribution:

$$W(\theta) = 1 + A_2 B_2 P_2\{\cos(\theta - \nu_0 t)\}$$

A_2 : Angular correlation coefficient
 B_2 : Orientation parameter

$A_2 B_2 = 7\%$ for 222 keV γ



($U_{\text{coeff}} = 0.749$)

$$R(t, \theta, B_0) = \frac{I(t, \theta, B_0) - I(t, \pi/2 + \theta, B_0)}{I(t, \theta, B_0) + I(t, \pi/2 + \theta, B_0)} \quad (\theta = \pi/4)$$

